

5.3 Leg M45/3

5.3.1 Moored Boundary Current Array at 53°N and Moored Observations at AR7-W

(J. Fischer, F. Schott, F. Morsdorf)

a) Recovery and Data Retrieval

The recovery of the 53°N boundary current array after the two years was a pleasant success. All 5 moorings were recovered and with the exception of one Aanderaa current meter and two acoustic current meters all (23 current meters) instruments had full 2 year-long records; mooring K19 was deployed for just one year as a continuation of mooring K9 that was recovered during VALDIVIA cruise V-172 (summer 1998). ADCPs and Seabird sondes worked without any data losses. Table 7.3.3 gives an overview of the available data that were almost finally processed at the end of the cruise. In fact, rapid processing, on board recalibration, and refurbishment of the instruments was necessary as most instruments were urgently needed for later deployments.

Three moorings (K27 - K29) were deployed at 53°N as another two year continuation of the boundary current array. Although horizontal and vertical instrument coverage had to be significantly reduced compared to the first period, first analysis of the data showed that the new array will cover the most prominent boundary current structures.

At the AR7-W section the continuation of the boundary current time series was successful by the recovery of mooring K22 (now K32 is in the water). Although the ADCP did not work; the rear plug had a shortage due to seawater leakage; the key timeseries at the 1500 m level is available, thereby extending the timeseries to now 3 years (K2/K12/K22).

b) The Boundary Current at 53°N; Preliminary Results for 1997 to 1999

The two-year-mean boundary flow clearly shows the mean structure of the boundary current (Fig. 42) and how it was resolved by the moored current meters. At the shelf break, mooring K7 and the upper part

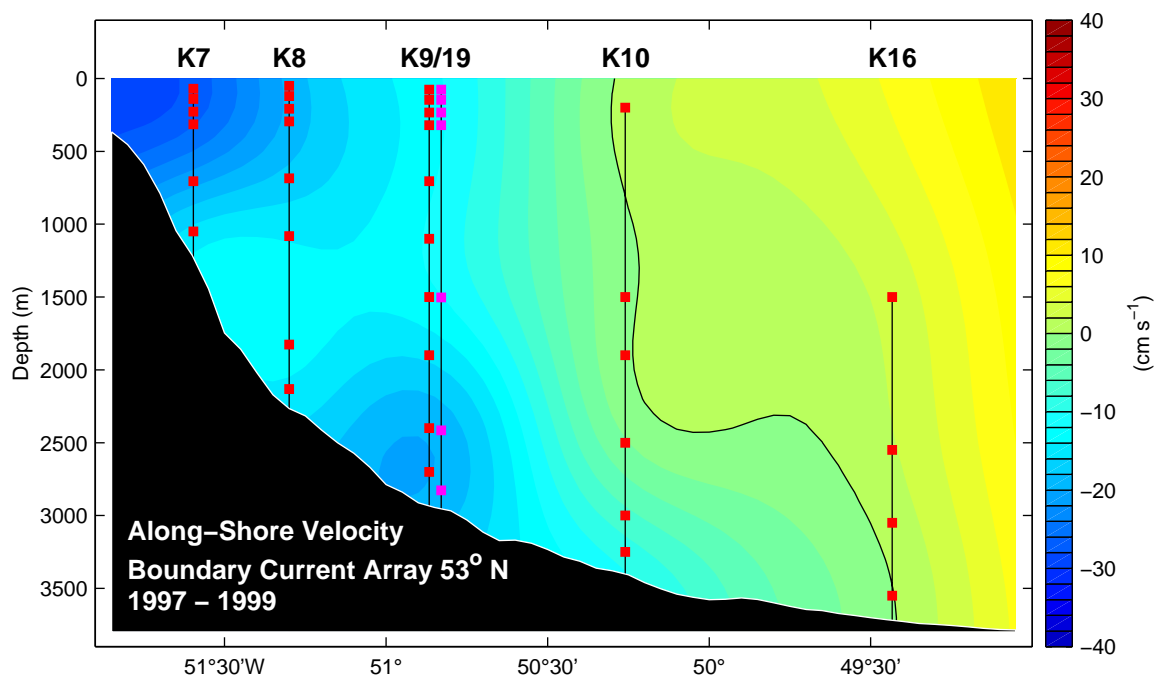


Fig. 42: Two year mean (summer 1997 to summer 1999) flow along the topography at 53°N. Mooring locations and instrumentation (current meters) are included. Mooring K19 is the continuation of mooring K9 with somewhat different instrumentation.

of K8 was within the shallow Labrador Current, that has some baroclinic structure in the top 1000 m of the water column. Farther out at K9/K19 the upper part of the water column has almost no shear, while near the bottom the maximum of the deep boundary current is found (more than 20 cm/s on average). Mooring K10 defines the outer edge of the boundary current, with some indications of the near bottom intensified flow to extend out to K16. For a preliminary transport estimate, we calculated the effective crossflow area for each of the instrument positions and by multiplying these areas with the measured flow at one day resolution and subsequent summation over all elements of the array we obtained at transport time series of the boundary current revealing large transport variability on timescales from days to weeks.

5.3.2 Convection Situation 1998/99 in ADCPs, T/S-Records

(F. Schott, C. Mertens)

a) Technical Aspects

Observations of deep convection were carried out at the moored stations K20 and K21, both deployed at Valdivia cruise 172 in summer 1998. Mooring K21 was equipped with a downward looking ADCP at 190 m depth, two additional current meters at deeper layers, and a number of temperature/conductivity recorders (SeaCATs/MicroCATs). All instruments were successfully recovered and had full records, thus extending the the time series of convection observations to now three years. After recovery the SeaCAT and MicroCAT recorders were lowered with the rosette and compared with the CTD measurements to check their long-term stability.

At mooring K20, located northwestward of K21, a moored CTD-profiler was installed. The profiler is designed to climb up and down the mooring wire while acquiring CTD data. Additionally mooring K20 was equipped with a downward looking ADCP as the top element. Except for some problems during the first two week after deployment, the moored profiler worked flawless until mid-January 1999. From then on, only the range below 1000 m was continuously covered. Thus the occurring convection activity was barely resolved.

b) Preliminary Results

The by now three year time series of observations in the central Labrador Sea revealed considerable variability of convection activity in this area. While deep convection reaching to depths of about 1500 m was observed during the winter of 1996/97, only moderate convection activity took place in the following winters. During the winter of 1997/98 a homogenization of the water column to a depth of about 600 m was observed, and the temperature records from the mooring K20 recovered during M45/3 show a penetration of the winter mixed layer to similar depths. Although the period of active convection is not covered by the CTD data obtained with the moored profiler at K21, profiles from mid-March indicate somewhat deeper mixing to about 1000 m at that location.

Corresponding to the weak mixing activity found in the temperature records, only few events of vertical velocity associated with convective plumes were captured by the ADCP measurements. Bursts of downward motion were observed between 22 and 28 February 1999, a period of relatively strong surface forcing according to NCEP/NCAR reanalysis data. Possible reasons for the weakening of convection activity in the Labrador Sea are the decrease of wintertime buoyancy loss at the sea surface (both winters 1997/98 and 1998/99 show means well below the 40-year average of NCEP/NCAR data), and the continuous warming observed in the temperature records over the three year period. The repeated CTD surveys carried out each summer, confirm that the warming is associated with increasing vertical stability of the Labrador Sea Water layer, thus counteracting the convection.

5.3.3 Tomography

(D. Kindler, T. Terre)

a) Technical Aspects

Recovery: During METEOR-cruise M45/3 two WEBB-type transceivers (400 Hz), one HLF5-type transceiver (250 Hz) and a French (IFREMER Brest) SARA-type stand-alone receiver were recovered safely, together with their releasable bottom-moored transponders. These ocean acoustic tomography instruments were deployed in August 1998 during VALDIVIA-cruise V172 in moorings K21, K22, K23 and K24, respectively.

The K21-transceiver had worked without technical problems during the whole deployment period of 340 days, yielding good receptions (in terms of the signal-to-noise ratio) from the strong HLF5-soundsource (see below) for most of the experiment time (see plot of acoustic intensity, Fig. 43). More than 5 early arrival groups can clearly be separated during winter. There are gaps in the arrival time series without any signal which are believed to be due to intense barotropic current events causing the receiving instrument of mooring K21 to subduct up to 900 m (Fig. 44).

During those events the ambient noise must be increased owing to surface noise and/or mooring induced noise which contaminates the receptions.

After the recovery of the K22-transceiver it turned out that there had been a leakage of the instrument's pressure housing obviously caused by a damaged connector in the upper end cap. This leakage resulted in a failure of the temperature and pressure sensor and in the weakening of the transmitter so that almost no signals were received at the other instruments. Nevertheless, clear receptions from K21 and K23 were recorded to K22 which will allow processing, even though only 2 of the 3 navigation channels had worked properly.

The HLF5 transceiver in K23 - for which substantial efforts had been taken to repair it in summer 1998, after it had failed because of a short circuit during the previous deployment - worked excellently for the whole year. Even with a reduced battery capacity, due to this failure, a high power level could be maintained until the end of its scheduled task. Both instruments in K22 and K23 showed much weaker mooring motion compared to the K21 instruments in the central Labrador Sea mooring.

The data retrieval of the SARA-type receiver in K24 showed that it had worked until mid June, i. e. it stopped a month earlier than scheduled for an already known technical problem. Environmental data like pressure and temperature had been correctly acquired. In a first processing of the reception data it appears that the signal-to-noise ratio was very low during the first 30 days, i. e. only late arrivals from K21 and K23 can be detected. After that there is no evidence of received signals from any source. Up to now there are only hypotheses for the faulty receiver. The most reasonable one claims that the upward looking omnidirectional hydrophone was too much contaminated by surface noise.

Re-deployment: The new ocean acoustic tomography array consists of three moorings, K32, K33 and K31, which were to be deployed in a triangle with side lengths of 210 km (K32-K33), 172 km (K33-K31) and 140 km (K31-K32) (Fig. 5). It follows the layout of the previous year by replacing K21 through K31 and K22 through K32, again using WEBB-type transceivers. One of these two had been prepared prior to the cruise, the other one was refurbished on board R.V. METEOR. The location of K33 was moved closer to K31 in order to reduce the distance as it contains a somewhat weaker WEBB-type sound source instead of the HLF5 (400 Hz compared to 250 Hz, previously). This instrument was the one with the leakage-induced problems (see above) which could be eliminated by replacing the damaged connector and changing some of the electronic modules. All WEBB-type instruments were programmed to transmit (and receive) signals 6 times a day for 2.5 to 5 minutes until 1 July 2000.

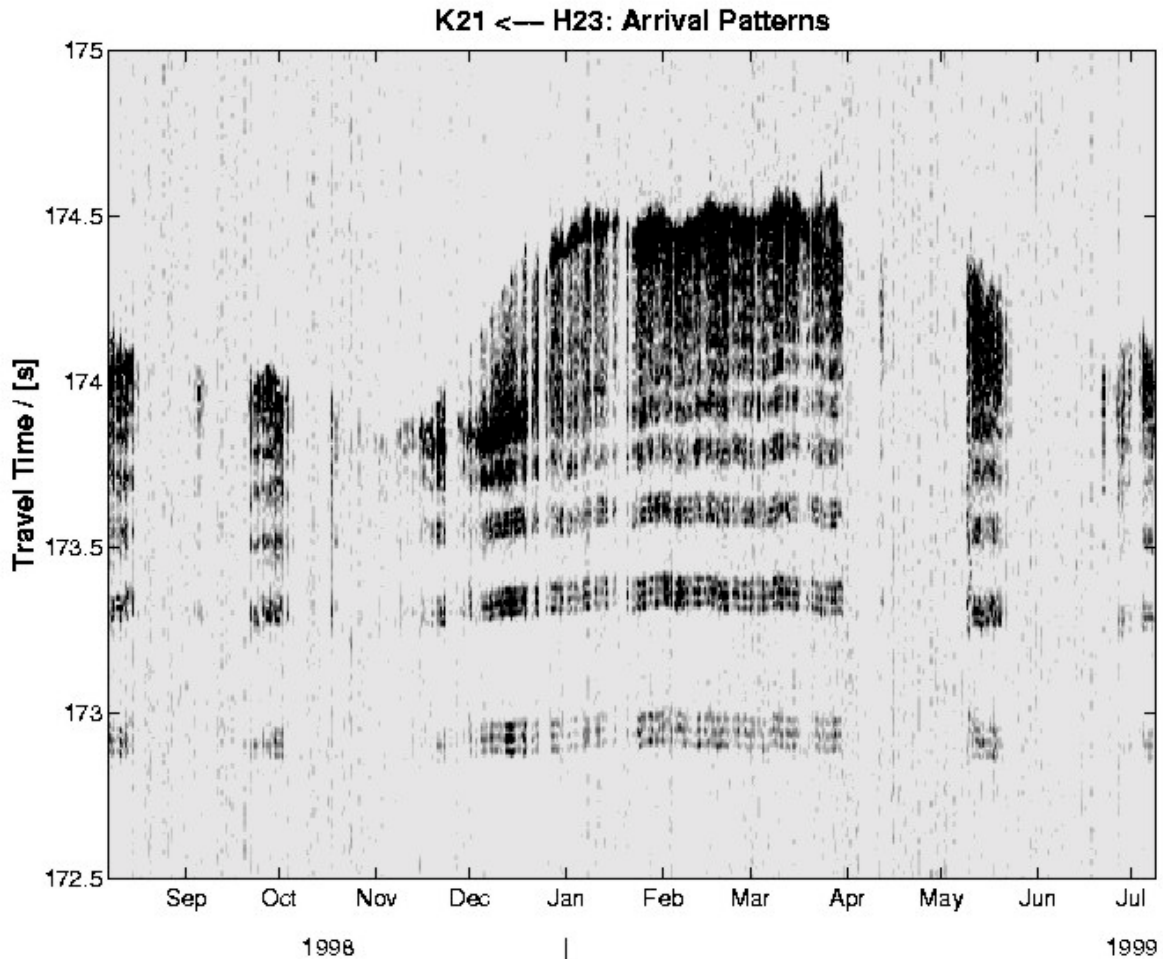


Fig. 43: Experiment timeseries of acoustic arrival patterns for the transceiver pair K21-K23 received by K21. The gray scale is a measure for the intensity of the received acoustic signal. Receptions are clock drift and mooring motion corrected.

Another French stand-alone receiver SARA was deployed in the same mooring (K33), more or less for testing purposes since the source of the erroneous receiver behaviour during the previous deployment could not clearly be detected. To protect its hydrophone against surface noise (a suspected source of error) the device was set deeper (240 m vs 120 m) with the hydrophone looking downward this time.

All moorings were supplied with three releasable bottom transponders each, in order to navigate the tomographic devices in the moorings for horizontal and vertical motions. The transponder positions were estimated by using differential GPS navigation and measuring their distances to the ship's transducer acoustically on different courses.

b) Preliminary Results

Receptions at mooring K21 from the strongest HLF5 sound source in K23 (over a distance of 255 km, Fig.5) could already be processed on board METEOR, after mooring motion and clock drift for both instruments had been determined, and eliminated. The resulting peak travel times were inverted into range-averaged sound speed profiles which then were translated into profiles of potential temperature.

From that, vertical averages for the upper 500 m and for a second layer between 500 and 1000 m depth were calculated. Their time series over the whole experiment are shown in Fig. 45, marked as dots. A comparison with the same property - estimated from hydrographic sections between K23 and K21

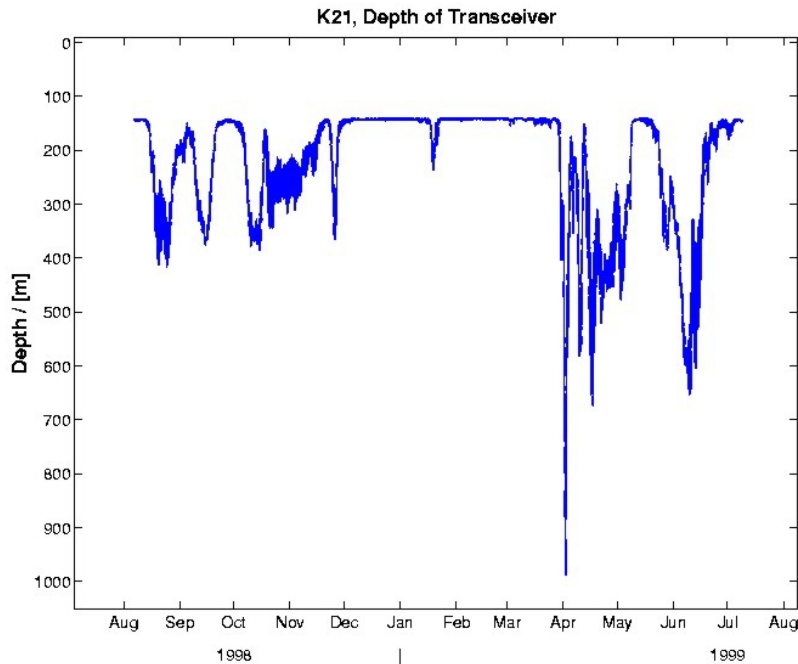


Fig. 44: Timeseries of transceiver depth, nominal deployment depth is 130 m. Subduction of the instrument is due to overleaning of the mooring caused by intense barotropic current events passing by the mooring position.

during the deployment and recovery cruise (marked by crosses at the at beginning and end of the temperature time series) - resulted in a good match.

A clear seasonal signal can be seen with an amplitude of about 0.4°C for the 500 m thick surface layer (Fig. 45, upper panel). It reveals a strong cooling, down from about 4°C in the beginning of November 1998 to 3.4°C in mid January 1999. During the winter until end of March it stays at low values slowly increasing afterwards and returning to its early November temperature in end of June.

The depth average for the lower layer (500 - 1000 m) is shown in the lower panel (Fig. 45). The seasonal signals don't seem to appear there. Only a slight warming trend over the duration of the experiment can be detected, confirmed by the hydrographic measurements.

These very first results already demonstrate the sufficiently good quality of the 1998-1999 tomographic dataset and that it can be successfully processed.

5.3.4 Water Mass Variability of the Labrador Sea 1998/99 vs Previous Years

(M. Rhein, L. Stramma, C. Mertens)

a) CTD and Oxygen Calibration (C. Mertens)

CTD profiles were made using a Sea-Bird SBE 9/11 system (IfMH SBE3) additional equipped with a Beckman dissolved oxygen sensor. The probe was attached to a 24 bottle 10 l General Oceanic rosette water sampler. Two bottles were left out for a lowered ADCP system, hence a maximum of 22 bottles was used throughout the cruise. Five bottles were equipped with electronic reversing pressure and temperature sensors, used to check the stability of the laboratory calibration. Within the accuracy of the reversing thermometers no deviations were found and no further correction to the laboratory calibration was applied.

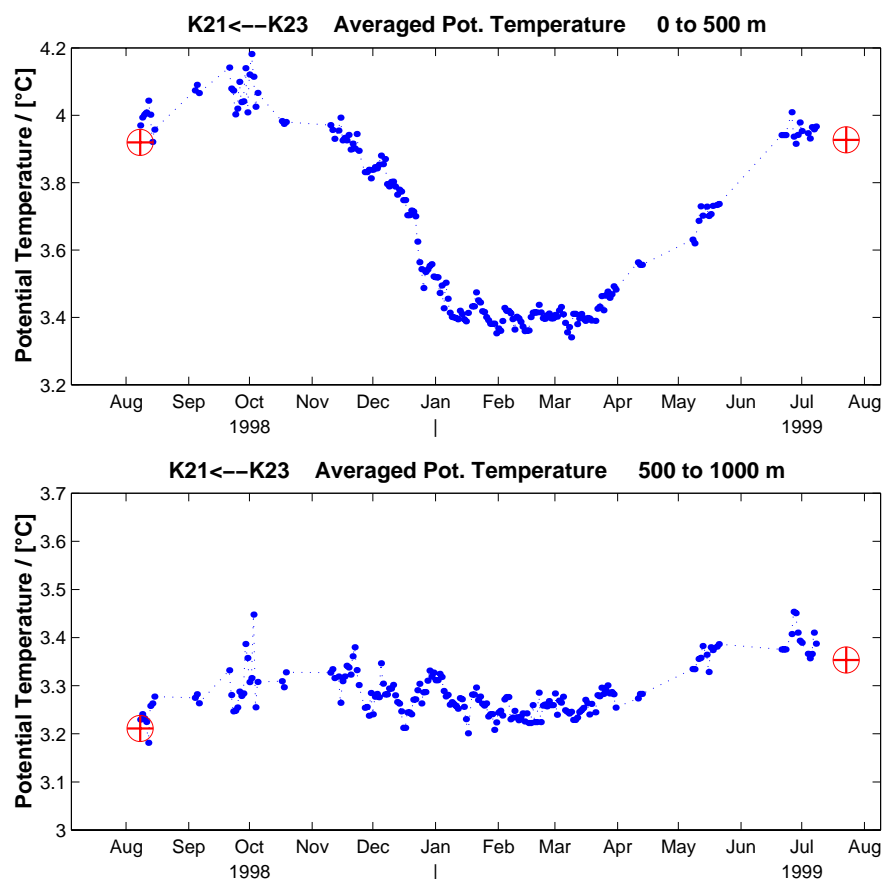


Fig. 45: Vertically averaged potential temperatures for depth intervals 0-500 m (upper panel) and 500-1000 m (lower panel). Dots: horizontal integral from tomography inversions for the mooring pair K21-K23. Crosses: same property as dots, but estimated from hydrographic sections (CTD-casts) between K23 and K21 at beginning and end of experiment, to demonstrate validity of acoustic measurements.

Salinity samples, typically four per profile, were analysed onboard using the new Guildline Autosol 7 salinometer. For the first two-third of leg M45/3 the salinometer worked fine with a time drift less than 0.001 in salinity during a measurement session. However, at the end of the cruise the stan by value became unstable from one probe measurement to the next probably to some salinometer electronic problems and had to be corrected additionally, however the corrected values were still usable for the calibration. The CTD salinities corrected by a pressure dependent offset fall within 0.0019 of the bottle samples.

Oxygen samples were analyzed by the marine chemistry group with traditional Winkler titration. On most stations samples were taken from all bottles plus double samples on some stations. Due to shift of the oxygen sensor response after a 3 day transit between CTD 44 and CTD 45, the calibration was done separately for the two periods. The coefficients for computing oxygen concentration from the CTD oxygen sensor were refitted, and a temporal drift as well as a pressure dependent offset were corrected afterwards. The rms-error is 0.040 ml/l for both legs.

For the first 13 CTD casts the system was build vertically into the rosette with no air bleed valve installed. Air trapped in the pumped system resulted in nearly useless downcast data especially in the thermocline due to strongly increased lags between temperature and conductivity sensor. Although an air bleed valve was installed after cast 13 some problems remained in strong vertical gradients, therefore the system was build horizontally into the rosette after cast 26. From then on the system worked properly for the remaining cruise. For the first stations upcast data have been analysed and appeared usable. A separate calibrations was computed for the upcast data, which gave similar accuracy as described above.

b) Tracer calibration (M. Rhein)

Chlorofluorocarbons calibration: 1550 water samples have been analysed on board with a GC-ECD technique. Accuracy of the data was checked by analysing 90 CFC-11 and CFC-12 samples twice and the mean rms was 0.7% for both components.

The CFC concentrations are reported on the SIO93 scale (R. Weiss, Scripps Institution of Oceanography, La Jolla, USA and calibrated against standard gas provided by D. Wallace (IFMK).

Carbontetrachloride: Additionally on this cruise, we analysed carbontetrachloride (CCl₄) in the sub-polar North Atlantic. The analysis procedure is similar to the one for CFCs. Major differences are the use of a capillary column for CCl₄ and different purge and trap materials and carrier gas fluxes. At the beginning of the cruise, the analysis suffered from a short time variability in the efficiency of the Electron Capture Detector (ECD). The measurements were successful at CTD profile 45 and afterwards. In total, 350 samples were measured. The accuracy based on replicate measurements was <1%.

c) Preliminary Results from Hydrography and CFCs (M. Rhein, L. Stramma)

The WOCE AR7W-section across the Labrador Sea was measured on the western half during cruises in July and August of 1999 as well as of the previous three years. The major water mass change in the Labrador Sea was the continuing descent of the isopycnal $\sigma_{\theta} = 27.74$ (the upper bound of Labrador Sea Water LSW) from 500 m depth in 1996 down to 1000 m depth. Additionally, the LSW defined to be limited by the isopycnals $\sigma_{\theta} = 27.74$ and 27.8 got warmer, saltier (Fig. 46) and CFC-poorer than found in the previous years. Owing to weakened convection intensity in the last winters the thickness of the LSW layer decreased from about 2000 m in 1996 to about 1300 m in 1999 (Fig. 46). Although the LSW layer was located at greater depth, the mean temperature increased from about 2.95°C in 1996 to 3.15°C in 1999 while the mean salinity increased from about 34.85 to 34.86.

During 1996 to 1999, the CFC-11 concentrations in the temperature minimum decreased from 4.4 pmol/kg (2.7°C) to 3.7 pmol/kg (2.85°C). These features indicate, that the density layer of LSW ($\sigma_{\theta} = 27.74$ to 27.80) was not ventilated by deep convection in the last winter. A closer look at the upper 1000 m showed that convection did not reach the $\sigma_{\theta} = 27.71$ isopycnal (about 600 m depth, $\theta = 3.2$ - 3.4 °C). One profile (CTD 25) along the WOCE AR7W section showed slightly lower salinities than the surrounding stations in the LSW layer, however the mean temperature and salinity distribution as well as the CFC measurements showed that it is not newly formed water, but remnants of older LSW. Compared to the previous years, the stability of the water column in the upper 1000 m increased, so that an onset of deep convection in the next winter requires higher heat fluxes than for instance in 1997. Further, south at the 53°N section, the amplitude of changes in LSW layer thickness, mean temperature and salinity reduced, but are still present. For example the thickness was about 1400 m in 1996, and only about 1200 m in 1999.

In 1999 the CFC-11 concentrations for the Gibbs Fracture Zone Water (GFZW) increased in the central Labrador Sea compared to the previous years. In the boundary current at 53°N and at AR7W no changes in the CFC values were found. The salinity of the GFZW in the central Labrador Sea was comparable to the 1996 conditions, i.e. more saline than 1997 and 1998. In the boundary current at 53°N, the salinities were generally lower than in the central Labrador Sea, and the interannual variability is as big as the scatter of one survey.

In the Denmark Strait Overflow Water (DSOW), the freshening and cooling since 1997 continued, and the salinity in the central Labrador Sea reached the 1996 level. At 55°N in the boundary region, however,

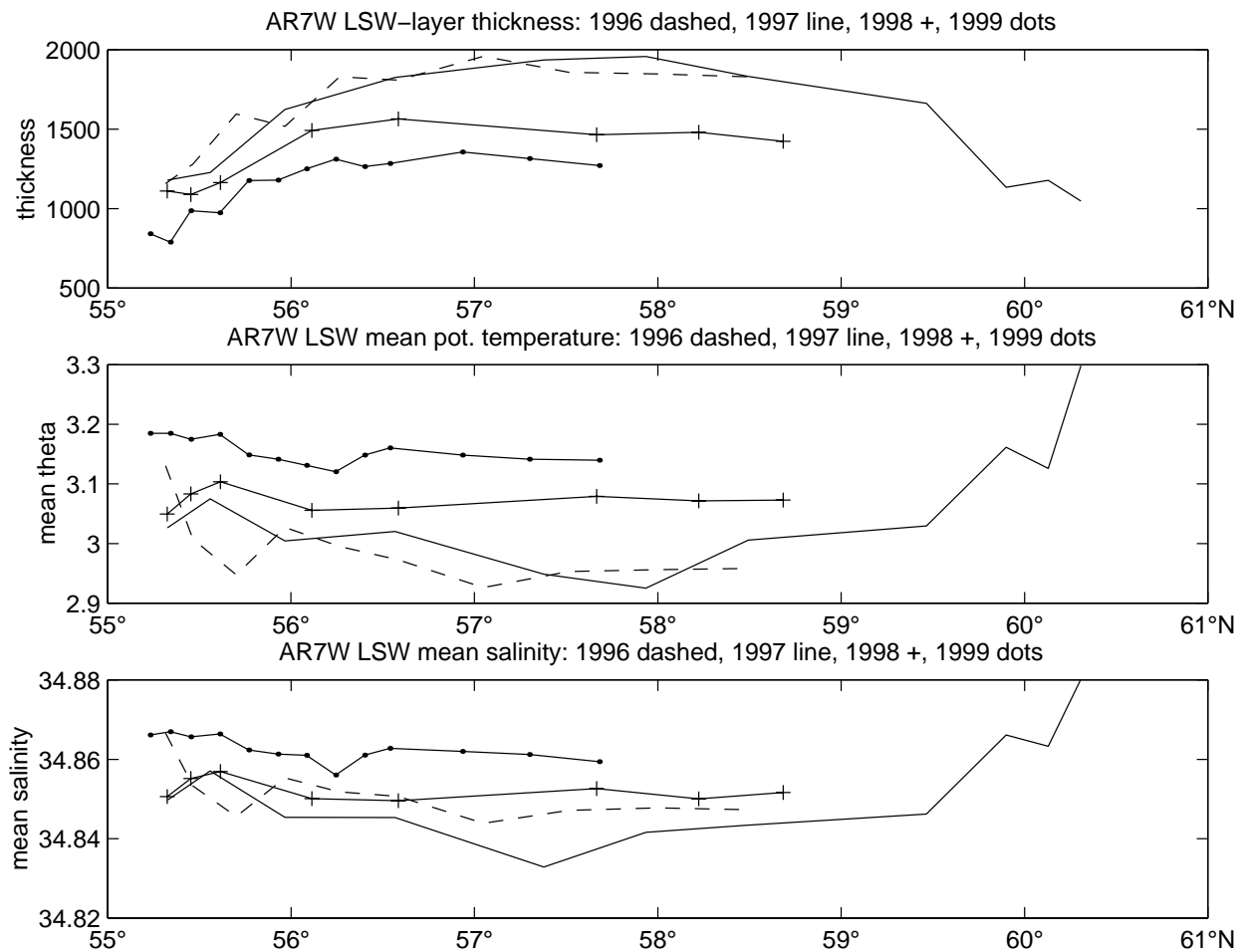


Fig. 46: Labrador Sea Water (between the isopycnals $\sigma_{\theta} = 27.74$ and 27.8) for the layer thickness in dbar (upper frame), mean potential temperature (center) and mean salinity (lower frame) for the summers of 1996 (VALDIVIA 161 dashed), 1997 (METEOR M39/4 line), 1998 (VALDIVIA 172 plus), and 1999 (METEOR M45/3 dots).

the 1999 DSOW was fresher and cooler than in 1997 and 1998 but not as saline as in 1996. At 53°N, the DSOW in 1999 is only slightly fresher than the 1997 and 1998 profiles.

5.3.5 Shipboard ADCP, LADCP and Pegasus

(J. Fischer, C. Mertens, P. Brand)

Technical aspects: A 75kHz ADCP was mounted in the ships sea chest for underway and on-station current measurements of the upper 600 m of the water column. Navigation for referencing the relative currents was of excellent quality due to differential GPS and almost 100% coverage by GPS-derived heading. The usual transducer misalignment could be determined quite well, so that the quality of the available data is pleasing. However, a large fraction of the data showed an intermediate layer (100 - 300 m) of very low backscatter; most likely caused by a depletion of plankton. The result was, that in some areas like the open Atlantic east of the North Atlantic Current, the ADCP range decreased drastically from over 600 m to less than 200 m. Nevertheless, the major sections (AR7-W, 53°N and the Grand Banks section) had sufficient data coverage mostly down to 600 m. During M45/3 a Linux based version of the

CODAS processing software was used for the first time, speeding up the processing by almost an order of magnitude.

Two LADCP versions were used during M45/3. During the first part of the cruise (in the Labrador Sea) the new LADCP2 version, two Workhorse ADCPs one up- one down looking, was used. Different from what was observed during its last usage (VALDIVIA 172) the compasses agreed well, so that we expected good data from this LADCP. However, some profiles looked spurious and there is more postprocessing needed.

During the second part of the cruise we used our standard LADCP that worked well during the rest of the cruise (station 45 to 104). The data were processed with two software versions, namely the well proven Fortran programs that were used during previous cruises and by a new MATLAB based version that includes an inverse procedure to determine the current profiles. The former procedure worked quite well and is the basis for the analysis products shown below; the latter procedure gave similar results in most cases, but some profiles could not be processed adequately with the new package.

PEGASUS casts were performed at the moored tomographic stations, where acoustic transponders were available. The intention of the Pegasus casts was to have a high quality comparison for the new LADCP2. Altogether six profiles were obtained in a region with almost barotropic flow that can be used for further comparison with the LADCP2 profiles. Some preliminary results of the LADCP measurements are presented in the next subsection.

5.3.6 DWBC East of the Grand Banks

(F. Schott, M. Rhein, L. Stramma, J. Fischer)

a) Array deployment, K18 results (F. Schott)

East of the Grand Banks, four moorings were deployed, the Deep-Water export Array, stations K101-1 to K104-1 (Fig. 5) and one mooring (K18) was retrieved that had been deployed in August 1998 during Valdivia cruise VA 172 south of Flemish Cap.

The Deep Water Export Array: The array as it was planned is shown in Fig. 47 superimposed on the mean boundary current as obtained by earlier measurements of the Bedford Inst. and U. Rhode Island groups. The four stations are designed to cover the major part of the southward- flowing cold water export and reach into the North Atlantic Current at the outer part. The deployment was carried out during 27-29 July after first doing HYDROSWEEP surveys around the potential mooring locations to beware against topographic distortions close to the mooring sites. Due to rough weather the topographic surveys were not too clean away from the immediate track line below the ship. The individual maps will have to be filled up during future cruises to arrive eventually at complete topographic charts from around the stations. Near the outer station, a first bottom survey yielded quite rough and curved topography so that it was decided to move that station further out on to a more gently sloping plateau, at 4300 m depth. All deployments went well.

Mooring K18: The water depth at that station was 4034 m, in the core of the lower Deep Western Boundary Current. Low-passed vector time series of the three current meters from near 1500 m, 3200 m and from 50 m above the bottom are shown in Fig. 48. The mean flow is southward at all depths, increasing from 4.3 cm/s at 1500 m over 9.0 cm/s at 3200 m to 12.3 cm/s near the bottom. There is strong variability in the currents at the weeks to months time scale. It is conceivable, from these records, that the current

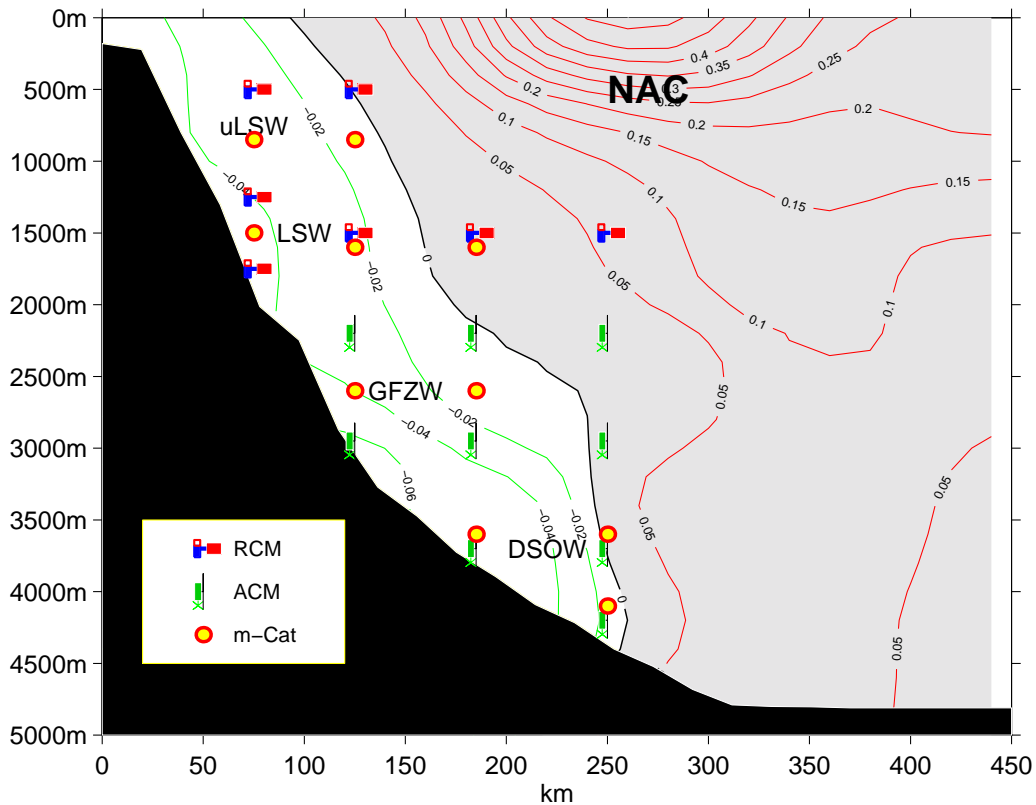


Fig. 47: Planned Deep Water export array of the Grand Banks; the underlying flow field is a 6-month average from the previous Canadian Array (curtesy Clarke/Meinen). Currents in m/s and NAC is for North Atlantic Current, DSOW for Denmark Strait overflow Water, GFZW for Gibbs Fracture Zone Water, LSW for Labrador Sea Water and uLSW for upper LSW.

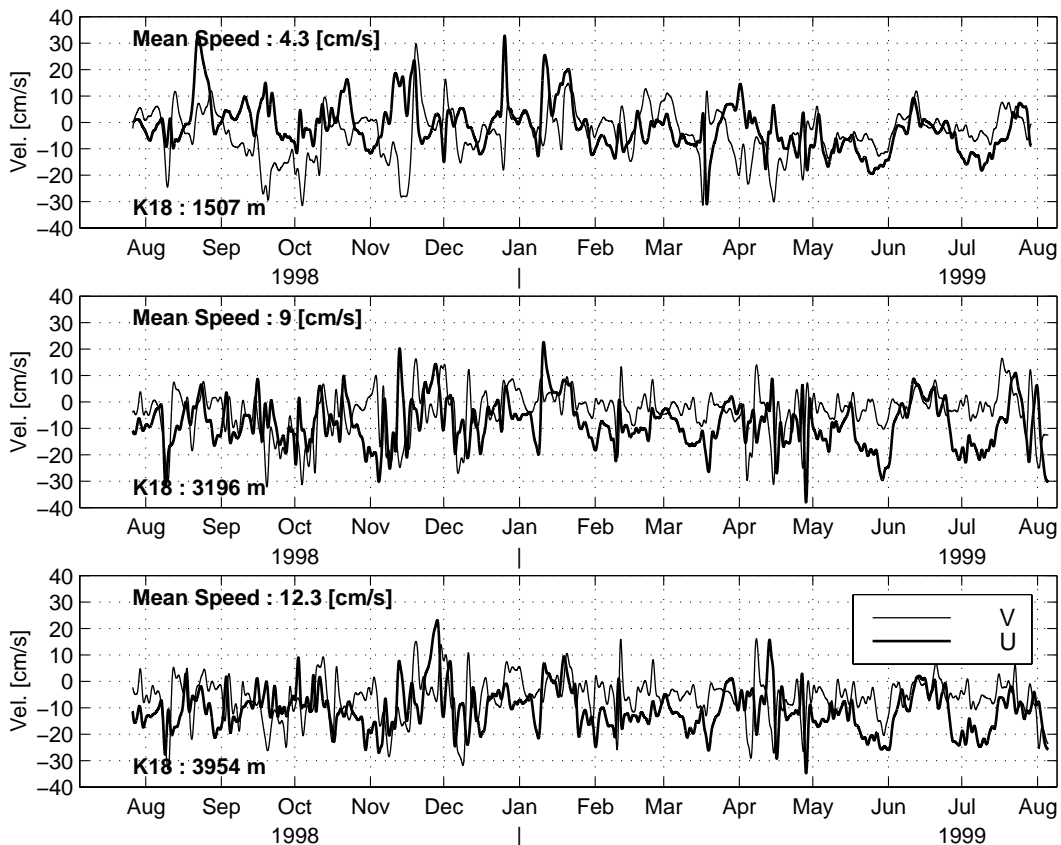


Fig. 48: Velocities of the three acoustic current meters in mooring K18, filtered with a 48 hour-cutoff lowpass. Thick line represents U, thin line V.

variability during the time of 11 days it took to close the box marked by CTD stations 45-87 could seriously impair the transport budgets over the box boundaries. What disappointed a bit was that no obvious T/S variability was recorded during the year by the Seacat instrument in the near-bottom layer.

b) Hydrography and CFCs (M. Rhein, L. Stramma)

The high resolution hydrographic section from the Grand Banks eastward at about 43°N was carried out to investigate the southward export of the deep water masses. This section is the western part of the WOCE A2 section, which was covered several times before from groups in Hamburg, although with a coarser horizontal resolution in the region of the DWBC.

The LSW bounded by $\sigma_\theta = 27.74$ and 27.80 has low salinities (Fig. 49) and high CFC concentrations (Fig. 50) at the continental slope. Additional lenses of fresh, CFC rich LSW were found at:

- a) 43.30°W (profile 65), where the high CFC core extends from $\sigma_\theta 27.60 - 27.67$, indicating water from the Labrador Sea presumably ventilated in 1997,
- b) 43-42°W (profiles 66-68) extending from $\sigma_\theta 27.78-27.84$, reaching well into the GFZW.

A low saline and high CFC mode of GFZW was also observed at 46°W (profile 60), although less distinct. In the GFZW, the CFC concentrations decrease with increasing salinity.

A first comparison of our section to the WOCE A2 observations of 1993, 1994 and 1997 off the Grand Banks (data from K.P. Koltermann for internal use) showed no obvious continuous changes in the LSW layer (σ_θ from 27.74 to 27.8) in layer thickness, mean temperature or mean salinity.

The densest water mass, the DSOW was present in three cores, the one with the highest CFC concentrations was located at 48°W in 3700 m depth. The other cores are located much deeper, at 4500 m (46°W) and at 4700 m (44 - 43°W). The densities of these DSOW cores are comparable, the isopycnals slope upwards along the continental slope. The salinity minimum at 45°W (Fig. 49) is accompanied by low CFC (Fig. 50), low CCl₄, and high silicate concentrations, and thus can not be DSOW, but northern reaches of Antarctic Bottom Water (AABW).

All deep water masses at Flemish Cap show compared to the Grand Banks section significantly higher CFC concentrations. The mean CFC-11 concentrations of LSW bounded by $\sigma_\theta = 27.74$ to 27.80 in the Labrador Sea is 3.6 pmol/kg. At the southern Flemish Cap section, the CFC values at the continental shelf are as high as in the Labrador Sea, but further west, the mean values are close to 3 pmol/kg. At the Grand Banks section, another 5° further south, only the 2 shallowest profiles close to the shelf have concentrations exceeding 3 pmol/kg. The values drop to 2.5 pmol/kg towards the west except for the two high CFC lenses (3 pmol/kg) mentioned above.

In the Labrador Sea, the mean CFC concentrations in DSOW are only slightly lower than in LSW. The concentrations drop to 2.5 pmol/kg at the Flemish Cap section and further south at the Grand Banks section, only 2 pmol/kg were found.

c) LADCP sections (J. Fischer)

Three sections with CTD/LADCP stations (Fig. 6) crossed the southward flowing western boundary current that was confined to the depth range inshore of the 4000 m isobath. For illustration of the mean flow pattern the barotropic (top to bottom mean) flow from all stations in the Newfoundland Basin is shown in Fig. 51. Offshore of the boundary current the northward flowing North Atlantic Current is seen in different intensities in the three sections. Moderate and narrow at the southern crossing and swift and broad at the southern Flemish Cap section.

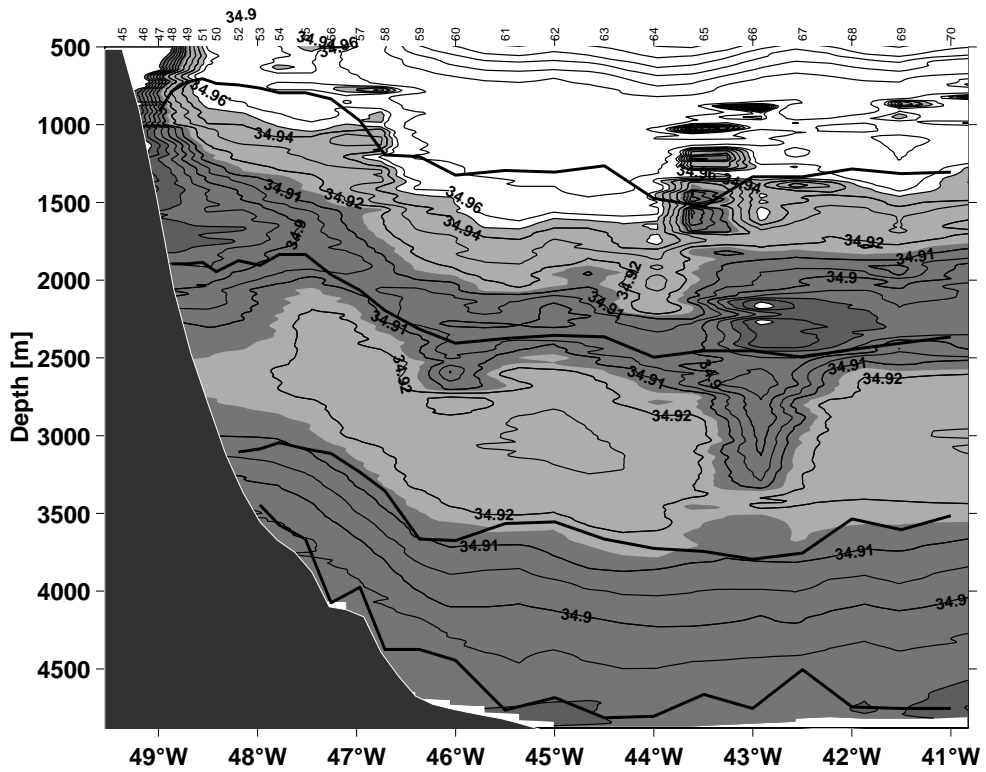


Fig. 49: Salinity distribution in the deep ocean along the 43°N section with dark shading for low salinities. The thick lines are $\sigma_\theta = 27.74, 27.80,$ and 27.88 which bound the deep water masses LSW (27.74-27.80) GFZW (27.80-27.88) and DSOW (>27.88). The deepest line is the isopycnal $\sigma_\theta = 45.90$, located in the core of the DSOW.

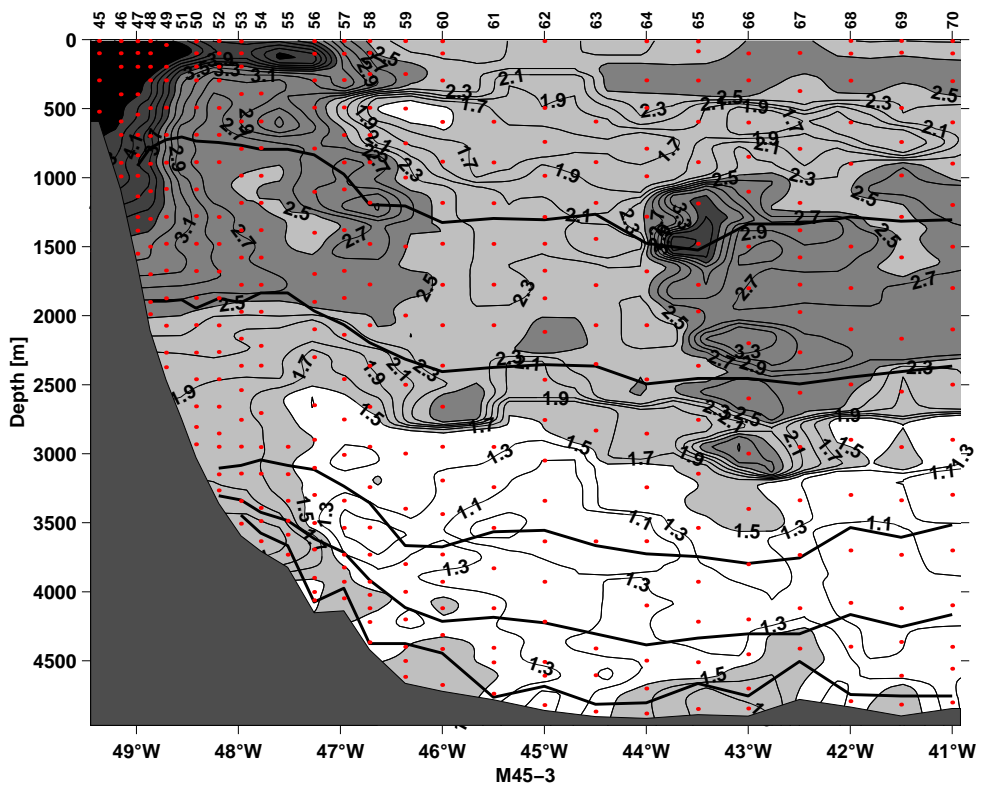


Fig. 50: CFC-11 distribution in pmol/kg (contour interval 0.2 pmol/kg, dark shading values) along 43°N section. The thick lines are $\sigma_\theta = 27.74, 27.80,$ and 27.88 which bound the deep water masses LSW (27.74-80), GFZW (27.80-88) and DSOW (>27.88). The two deepest lines are the isopycnals $\sigma_\theta = 45.885$, which is the upper bound of the high CFC core of DSOW and $\sigma_\theta = 45.90$, located in the core of the DSOW.

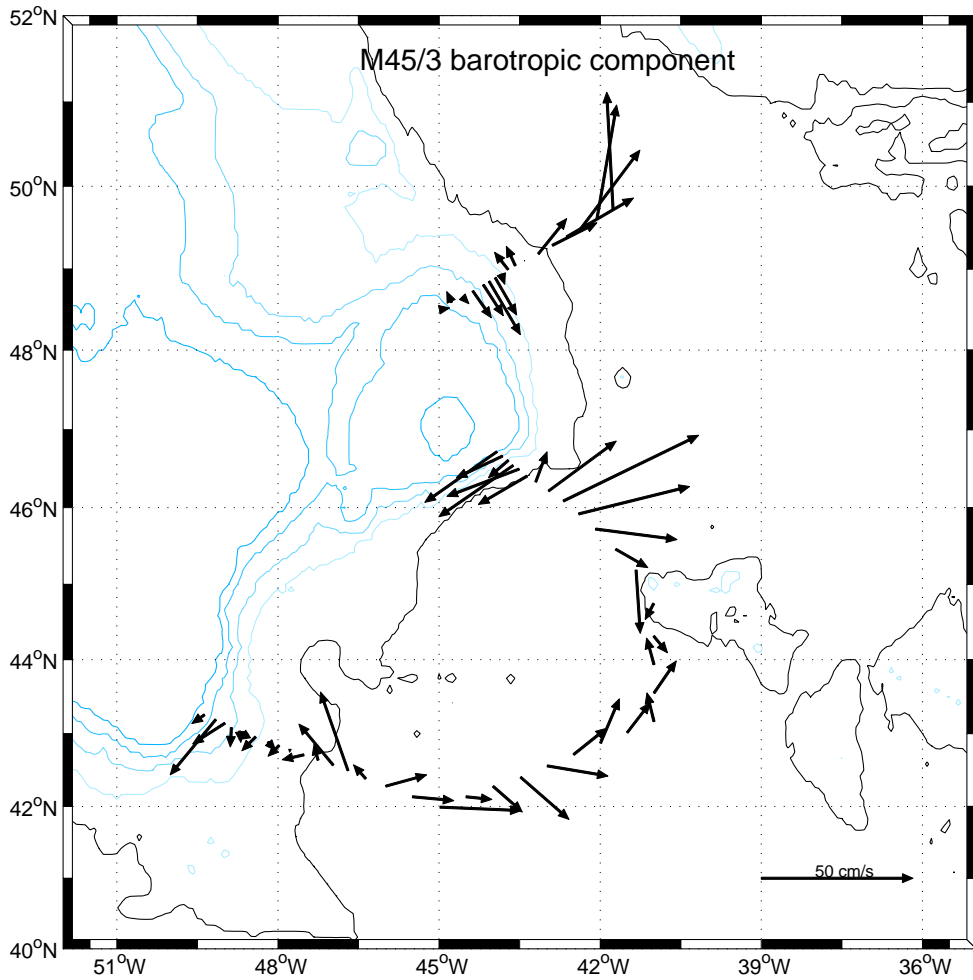


Fig. 51: Vertically averaged (top to bottom) currents from LADCPs on stations 45 to 104; for scaling see vector in lower right corner.

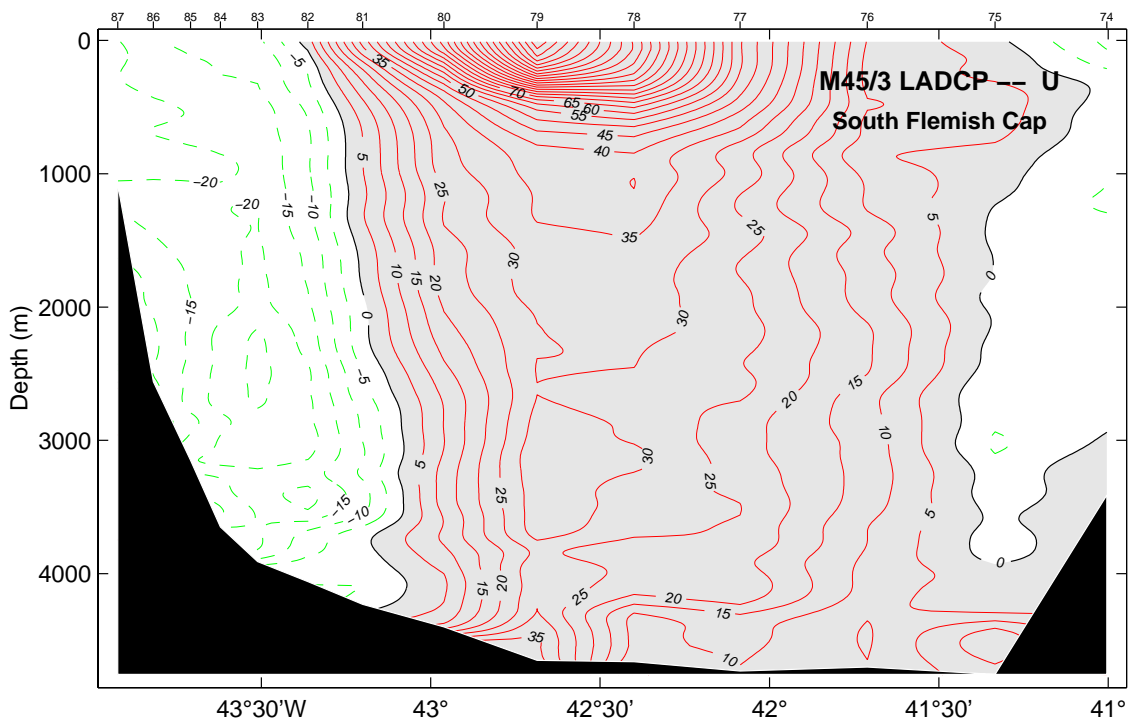


Fig. 52: LADCP section near 46°N (South Flemish Cap section) showing the zonal current component (shaded is eastward); velocity in cm/s.

The most impressive example of the flow is seen in the South Flemish Cap section (Fig. 52), at a location where the topography is steepest. There the southwestward boundary current is only about 60 km wide with almost barotropic flow of up to 20 cm/s. Offshore of the boundary current, the North Atlantic Current (NAC) covers about 100 km. Maximum near surface flow is nearly 170 cm/s with the current extending down to the bottom at 4700 m depth. In the center of the jet the vertically averaged flow extends 40 cm/s, and as a consequence the NAC transport was of the order of 150 Sv.

5.3.7 Marine Chemistry

(K. M. Johnson, K. Friis, F. Malien, T. Steinhoff)

Marine Carbon Dioxide System, Dissolved Oxygen, Nutrients, ¹³C and ¹⁴C

In continuation of leg M45/2, the working program on leg M45/3 followed the same four independent methods for detecting and estimating the oceanic CO₂-uptake in the North Atlantic. For general aspects and technical details see Section 5.2.5.

5.3.7.1 Total Dissolved Carbon Dioxide

As on M45/2, most of the samples drawn for DIC determination were not poisoned with HgCl₂, and the unpoisoned samples were always analyzed within 24 hours of collection. However, because a longer time between collection and analysis was anticipated for samples collected at stations 409, 424, and 465 the samples were poisoned with 0.05 mL of a saturated solution of HgCl₂. A total of 712 individual water samples from 37 stations along with 69 duplicates were analyzed during M45/3 (n = 781). In addition, 49 Certified Reference Material (CRM) and 39 „over determination samples“ (see Section 5.3.7.6 below) were analyzed for a total of 869 analyses.

The DIC analysis were made by SOMMA-Coulometry as described in Section 5.2.5.1 with one change in procedure. For M45/3, a conductance cell (Sea Bird Model SBE-4) was incorporated into the SOMMA system as described by JOHNSON ET AL. (1993). Hence salinity was measured on each sample analyzed which added 1 to 3 minutes to each DIC determination. The mean difference and standard deviation of the mean difference between the SOMMA-based salinity and the CTD salinity is 0.010 ± 0.154 (n = 780).

Aboard ship the system was again calibrated by analyzing Certified Reference Material (CRM) bottles which contain seawater with a known or certified DIC concentration. The CRM were prepared by Dr. Andrew Dickson and analyzed by Dr. C. D. Keeling by vacuum extraction with manometric detection at the Scripps Institution of Oceanography in La Jolla, CA. Lastly, gravimetric determinations of the sample volume (V_T) at 20 °C were made before the cruise, in St. John's prior to the start of the M45/3 work, and on 7 August aboard ship at the completion of the work. The ship board samples will be weighed in Kiel and corrections to the pre-cruise sample volume (V_T) will be made if necessary and DIC will be recalculated using the corrected V_T as part of our quality control and assurance procedure. Likewise the salinity data will be evaluated for significance differences between SOMMA-based and ship-based salinities to ensure that our sample depths correspond to the bottle closure depths, and the final DIC will be calculated with the ship-based salinity. The System Performance is given in Table 7.

Table 7 indicates very stable system performance over the two legs. There is some evidence for an increase in sample imprecision and a small loss of CRM accuracy for M45/3. The CRM results are consistent with previous experience (JOHNSON ET AL., 1998) where over time and repeated analyses the sample pipette becomes dirty and the sample volume (V_T) decreases slightly. The pipette calibrations

Tab. 7: Accuracy and Precision of SOMMA-Coulometer system 032 during the M45/3 Cruise. Part I: Accuracy based the analysis of the CRM. Part II: Precision from the duplicates collected for 69 of the 712 Niskin bottles sampled. Sample precision is given as the mean absolute difference between duplicates. The duplicates were either analyzed on the same day collected (with the same coulometer cell) or on a different day usually the day after collection with a different cell. Standard deviations are indicated by the \pm symbol. The corresponding results from leg M45/2 are shown for comparison.

Part I. Accuracy (Analysis of the CRM from Batch # 45)			
Analyzed (no.)	Mean DIC ($\mu\text{mol kg}^{-1}$)	Certified DIC ($\mu\text{mol kg}^{-1}$)	Mean Diff. ($\mu\text{mol kg}^{-1}$)
45/349	1993.50 \pm 1.52	1994.17 \pm 0.93	- 0.67
45/236	1993.85 \pm 1.55	1994.17 \pm 0.93	- 0.32
Part II. Precision (CRM and 50 sample duplicate pairs)			
CRM	All Duplicates (n) mean ($\mu\text{mol kg}^{-1}$)	Same Day (n) mean ($\mu\text{mol kg}^{-1}$)	Different Day (n) mean ($\mu\text{mol kg}^{-1}$)
45/31.52 (49)	1.06 (69) \pm 0.97	0.94 (35) \pm 1.00	1.19 (34) \pm 0.94
45/21.55 (36)	0.80 (50) \pm 0.64	0.64 (35) \pm 0.51	1.17 (15) \pm 0.77

made at sea (see above) should allow us to correct for changes in V_T . The increase in sample imprecision without a concomitant change in the precision of the CRM analyses may also indicate a change in sampling procedures during M45/3 compared to M45/2. Clearly the sample precision, particularly the different day samples, indicate that biological changes in the unpoisoned sample bottles did not occur or if they did they were too small to measure. Based on these results the overall quality of the data set is expected to be high.

A preliminary plot of DIC vs. pressure from stations 402 through 481 is shown in Fig. 53. The cruise structure was such that the DIC data can be divided into samples from the Labrador Sea (or Northern Phase, Stations 402 - 446) and a second set of data from the Newfoundland Basin (Southern Phase, Stations 448 - 481). The Northern Phase results are characterized by much greater uniformity than those of the Southern Phase where greater variability at pressures less than 2000 dbar arises due, apparently, to the mixing of water masses. See Section 5.3.7.2 for further discussion.

5.3.7.2 Spectrophotometric pH_T Determination

In addition to DIC, pH (on the total scale = pH_T) was measured on the same samples. A total of 869 samples were analyzed ($n = 795$). The samples were taken and analyzed in the same way as described in the M45/2 section 5.2.5.1 The short term and long term precision of the pH determination is based on replicate measurements on each station and on daily CRM (see above) measurements, respectively. For short term precision estimates, we measured the replicates normally in the beginning and at the end of a measuring cycle of a station. The running mean difference derived from 53 replicate measurements from station 402 to station 471 is ± 0.002 pH units. The long term precision within this period was ± 0.0015

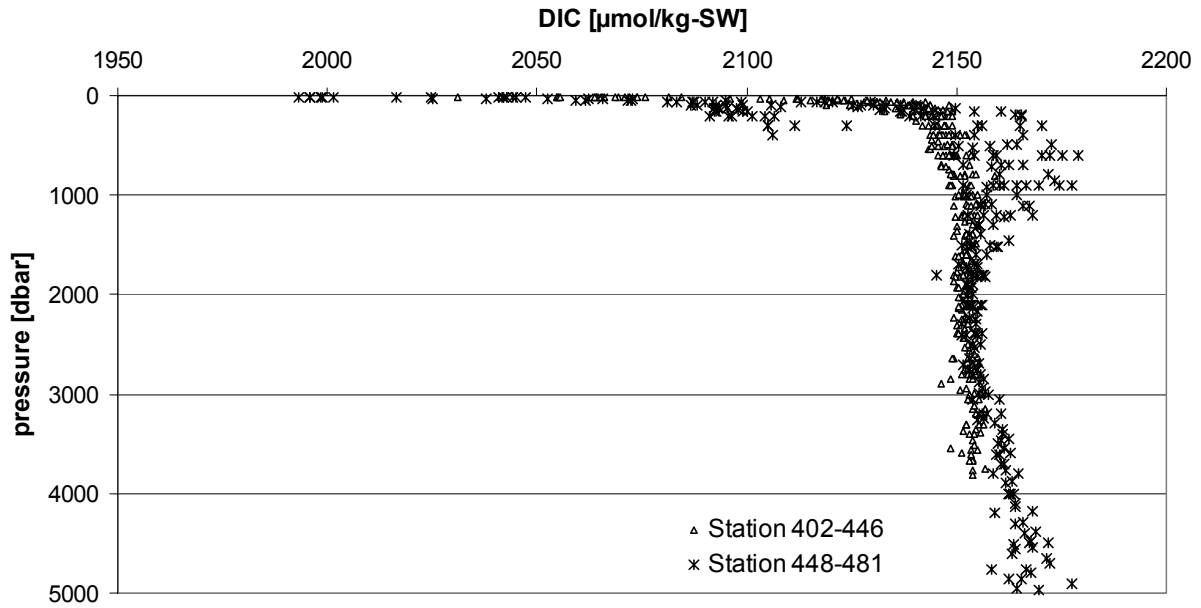


Fig. 53: DIC data from the Labrador Sea (Station 402-446) and the Newfoundland Basin (Station 448-481).

($n = 24$) pH units. The measured pH_T from CRM Batch # 45 was corrected according to DELVALLS AND DICKSON (1998) and is 7.9391 ± 0.0015 . The measured precision is in the range of the expected yearly decrease in pH due to the increase in atmospheric pCO_2 from fossil fuel combustion, deforestation etc.

The pH_T vs. pressure profiles from stations 402 to 481 are compiled and given in Fig. 54. The shape of the pH plot in general has been explained before (see Section 5.2.5.1 for M45/2). Fig. 54 clearly shows the relatively homogenous pH values with depth on the transects through the Labrador Sea (Stations 402 - 446). High pH values from about 2700 dbar to the bottom should be the signature of the Denmark Strait Overflow Water. The cold DSWO has, due to its formation history, a low pH. Much more variability is observed on the southern most profiles (Stations 448 - 481), which is due to mixing of two

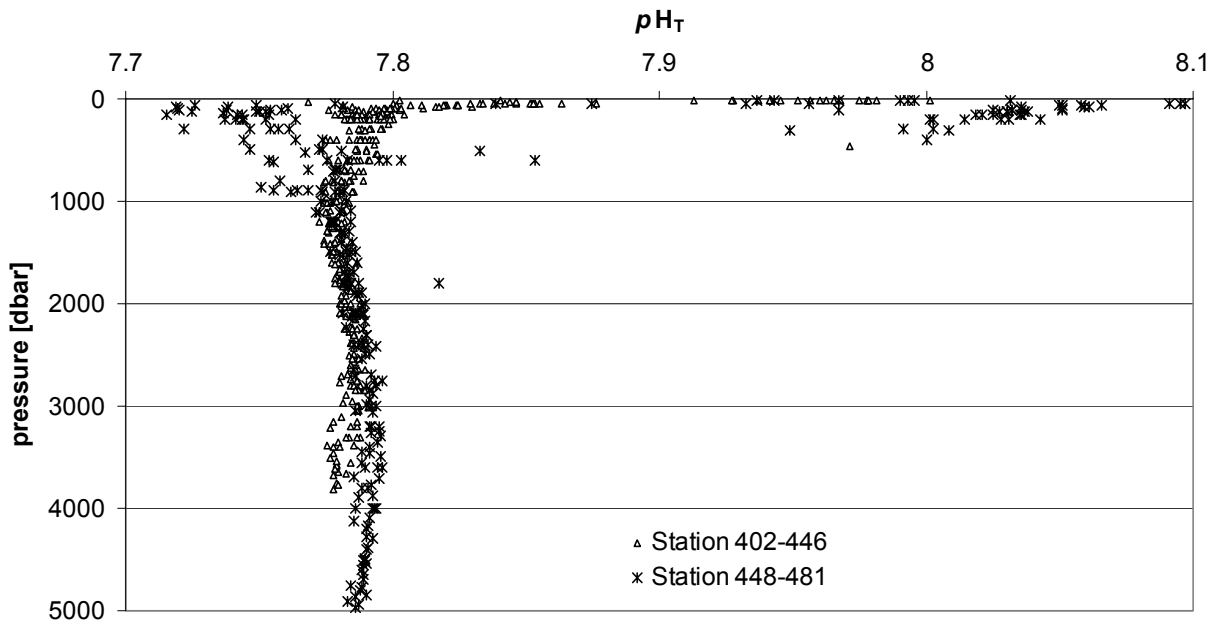


Fig. 54: pH_T ($T=22.00^\circ C$) data from the Labrador Sea (Station 402-446) and the Newfoundland Basin (Station 448-481).

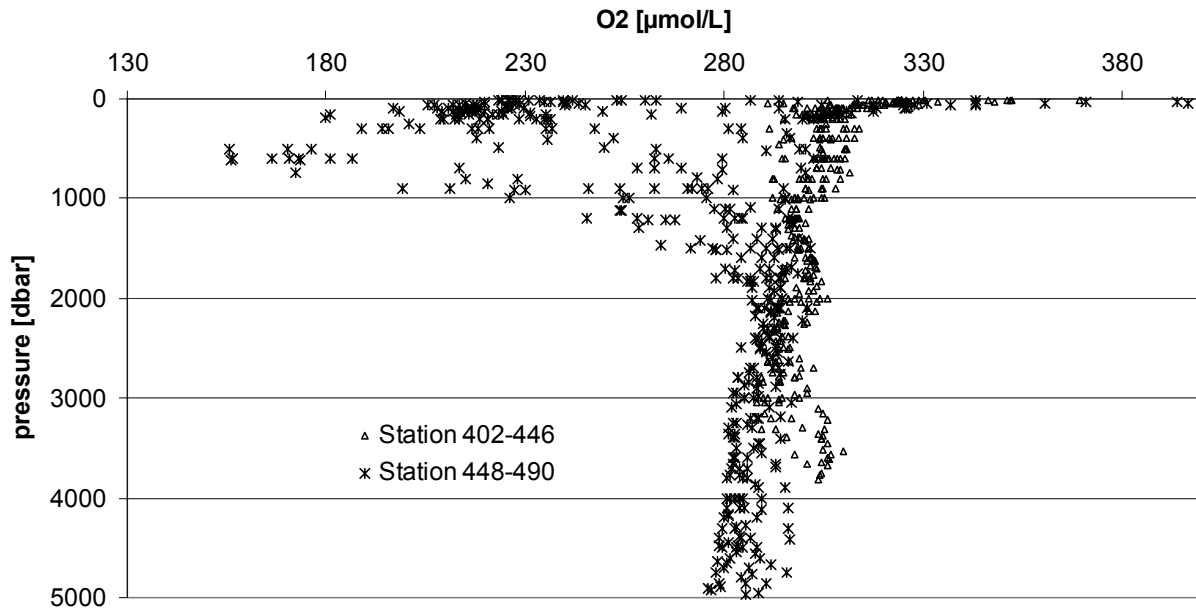


Fig. 55: Oxygen data from the Labrador Sea (Station 402-446) and the Newfoundland Basin (Station 448-490).

water masses with totally different DIC signatures, the North Atlantic Current and the Labrador Sea Water. The same variability is observed in the CO_2 correlated parameter oxygen (Fig. 55).

5.3.7.3 Nutrients and Oxygen

Nutrients (nitrate, nitrite, phosphate, silicate) and oxygen were measured according to the same procedures described for M45/2 in Section 5.2.5.1. A total of 1401 samples from Niskin bottles were determined for nitrate, nitrite, phosphate, and silicate with an accuracy of 0.205, 0.005, 0.025, and 0.5 $\mu\text{mol kg-SW}^{-1}$, respectively. Oxygen was determined on 1313 samples collected from Niskin Bottles. Precision, estimated from the mean difference between replicate measurements for 29 randomly selected samples, is $\pm 0.28 \mu\text{mol kg-SW}^{-1}$.

5.3.7.4 Sea Surface $f\text{CO}_2$

As on Cruise M45/2 we measured the fugacity of CO_2 along the entire M45/3 cruise track. But in contrast to the M45/2 results (Fig. 39), we found sea surface over saturation in $f\text{CO}_2$ during M45/3 as shown in Fig. 56. The measured over saturation occurs on the transit transect from the Labrador Sea to the Newfoundland Basin. The southward flowing Labrador Current becomes warmer through heat gain from the atmosphere and through mixing with the warm North Atlantic Current. Due to the non-linear decrease in CO_2 solubility with increasing temperature the southward flowing water becomes over saturated by up to 115 %. (The solubility decrease is approximately 4 % per degree C increase.)

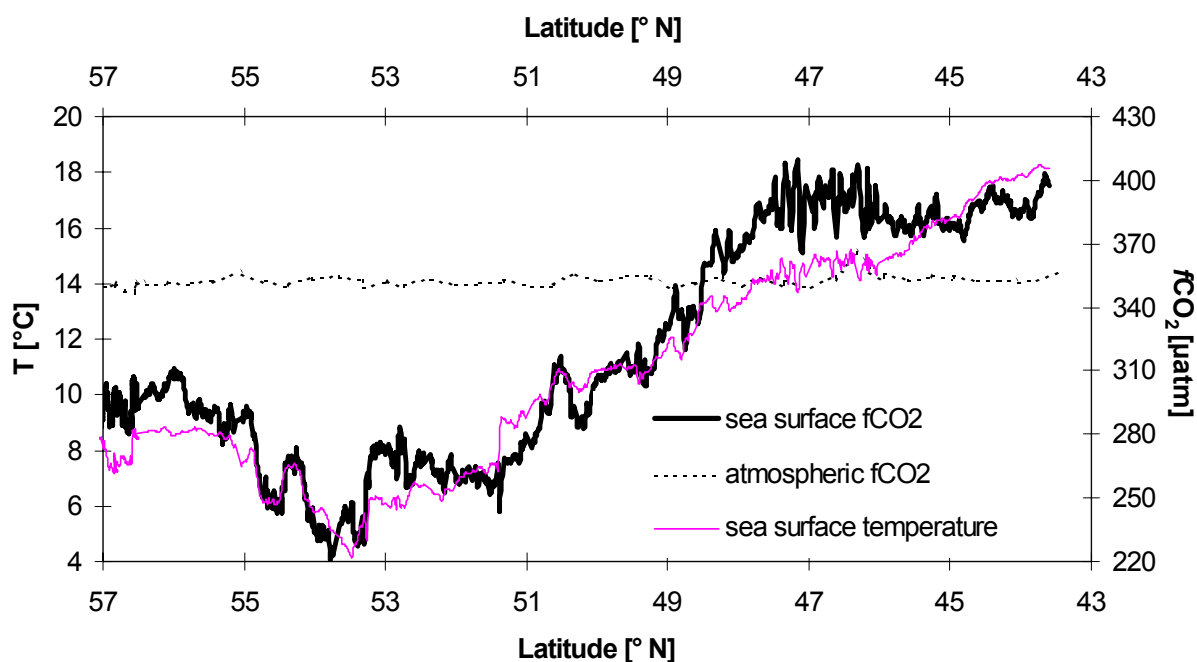


Fig. 56: Fugacity of CO₂ on the north-south transit from the Labrador Sea to the Grand Banks.

5.3.7.5 Carbon Isotopes

¹³C : On leg M45/3, 374 samples on 19 stations were collected for on shore ¹³C analysis. The sampled locations are listed in 7.3.4.

¹⁴C: On M45/3, 3 historical ¹⁴C (also ¹³C) hydrocast locations were repeated as shown in Table 8.

Tab. 8: M45-locations near to historical (previously sampled) stations with number of ¹⁴C samples collected

M45/3		GEOSECS		TTO	
424	22			193	13
485	22	27	20	228	18
490	22			224	16

5.3.7.6 Determination of the Carbonate System

In marine carbonate solution chemistry any pair of parameters (e.g. DIC and pH) can be used with the dissociation constants for carbonic acid to calculate the other two parameters (in this case Alkalinity and fCO₂). For these calculations, several different sets of dissociation constants are available and routinely used. Ideally, for ocean CO₂-uptake calculations with the classical CO₂ parameters it should be clear which set of dissociation constants is the best. However, there is still no agreement as to which set should be used. The determination of more than 2 of the 4 parameters on the same sample is defined as over determination. Uniquely, the Kiel CO₂ Group possesses the ability to accurately measure all four classical carbonate system parameters. Hence M45/2 and M45/3 afforded us the opportunity to over determine the carbonate system and to evaluate the constants. For his purpose, we took 130 replicates for DIC, pH and alkalinity (stored for on shore measurement) from 6 hydrocasts on M45/2 and M45/3. In addition, we

took 39 samples from our pCO₂ underway system for DIC, pH, alkalinity and *f*CO₂. Using these data we should be able to empirically fit the data such that an empirical proof and a recommendation for the best set of constants will be possible.

5.3.8 Tritium/Helium Sampling

(R. Hohmann)

During the M45/3 course, a total of 180 samples for helium isotope analysis (Tab. 9), and 163 samples for tritium analysis were collected along a section across the continental slope near the Grand Banks extending from 43.2°N/49.2°W to 42.0°N/45.0°W. The samples will be analysed at the Noble Gas Laboratory at Lamont-Doherty Earth Observatory of Columbia University in Palisades, NY.

Compared to the classical hydrographic parameters, helium and tritium provide complementary information for water mass analysis making them a valuable tool to study the time scale of oceanic processes. Making use of the well known input history of ³H at the ocean surface and its radioactive decay to ³He, the distribution of ³H and ³He can be used to calculate the apparent ³H-³He age which is a measure for the time elapsed since the water mass was isolated from the atmosphere. It can be used to estimate formation rates and spreading times of the most prominent water masses. The interpretation of the ³H and ³He data will be done with respect to the results from ³H-He time series data obtained from the Labrador Sea since the beginning of the 1990's.

Tab. 9: Helium (He) and Tritium (Tr) samples taken during M45/3

Station	CTD	Longitude [°W]	Latitude [°N]	He samples	Tr samples
449	46	49.155	43.195	8	7
450	47	48.992	43.140	9	9
451	48	48.866	43.080	10	9
452	49	48.711	43.037	11	10
454	50	48.417	42.956	16	12
457	53	47.975	42.840	13	11
458	54	47.780	42.788	16	14
460	56	47.257	42.640	19	16
462	58	46.714	42.477	19	18
463	59	46.365	42.384	19	19
466	61	45.500	42.134	20	19
467	62	44.999	42.000	20	19

5.3.9 Air-Sea Exchange Observtions (M. Coldewey)

To investigate the interaction between ocean and atmosphere meteorological measurements were made on this part of the cruise. On the port side of the foremast in a height of 16 metres three instruments for flux measurements were installed. The wind fluctuations in three components were registered with 30 Hz by an

ultrasonic anemometer. A psychrometer measured the dry and moist air temperature with a frequency of 5 Hz. The pitch and roll of the vessel was also recorded. With the third instrument 10 Hz measurements of the fluctuations of humidity were made. In addition to the foremast, on the flybridge deck, a 19GHz radiometer was installed at the rail to get the sea surface temperature.

5.3.10 DVS-and Thermosalinograph Observations

(L. Helmbrecht)

A set of navigational, meteorology and oceanography data has been extracted from the R/V *METEOR*'s data distribution system for the duration of M45/3. For further distribution to the participating scientific groups the data is available as plain ascii file or a set of Matlab files. Further a Matlab Toolbox was created for easy data access and processing, including some basic visualisation tools. Data from the ships thermosalinograph has also been recorded for M45/3. For calibration of temperature and salinity the near surface data from CTD were taken. The attempt to calibrate the salinity with samples taken directly from the thermosalinograph was aborted, since the samples were quite dirty and would have polluted the laboratory salinograph.